Hindawi
Shock and Vibration
Volume 2022, Article ID 4186791, 9 pages
https://doi.org/10.1155/2022/4186791

Research Article

Determination of Width of Sectional Coal Pillars in the Working Face of Burst-prone Inclined Thick Coal Seams

Sitao Zhu,[1] **Gaoang Wang**,[1] **Kuiming Liu**,[2] **Jinhai Liu**,[3] **Fuxing Jiang**,[1] **Chun Zhu**,[2] **Xiao Wang**,[4] **and Yu Zhou**[5]

[1]*School of Civil and Resource Engineering, University of Science and Technology Beijing, Beijing 100083, China*
[2]*State Key Laboratory for Geomechanics & Deep Underground Engineering, China University of Mining & Technology (Beijing), Beijing 100083, China*
[3]*Hebei State Key Laboratory of Mine Disaster Prevention, North China Institute of Science and Technology, Beijing 101601, China*
[4]*School of Civil Engineering, Southeast University, Nanjing 211189, China*
[5]*Engineering Research Center of Geothermal Resources Development Technology and Equipment, Ministry of Education, Jilin University, Changchun 130026, China*

Correspondence should be addressed to Kuiming Liu; liukm1996@126.com

Received 9 May 2022; Accepted 29 June 2022; Published 19 September 2022

Academic Editor: Yonggang Zhang

In coal mines, a reasonable design of the widths of coal pillars is critically important, particularly for rockburst mines. This is because the frequent occurrence of rock burst in coal mines often arises from the inappropriate widths of the coal pillars. To address this problem, we first review two recent incidents of rockburst occurring and thus present a theoretical calculation of lateral bearing pressure distribution in goaf of inclined thick coal seam to illuminate the occurrence mechanism of rockburst induced by inappropriate width of sectional coal pillars. Based on the mechanism model, we then propose a design criterion for sectional coal pillar widths in inclined thick coal seams that can effectively reduce the risk of the induced rock burst. Our theoretical calculations, field stress monitoring, numerical simulation and field investigation all demonstrate the validity of the proposed design criterion in preventing the induced rock burst and large deformation of surrounding rock. The results from this paper may be used as a theoretical guidance of sectional coal pillar designs in inclined thick coal seams.

1. Introduction

Inappropriate width of coal pillars is an important factor that induces rockbursts in the working face along the goaf [1–3]. At present, in the central and eastern part of China, narrow coal pillars are used to protect roadways along the gob in mines with a depth of more than 600 m. However, In Xinjiang, Inner Mongolia, and Shanxi provinces, mines with depths between 300 m and 500 m still protect roadways with 15 m to 30 m wide sectional coal pillar, which are typically used in shallow mines. In the process of mining the working face, the mine pressure of roadway along the goaf is strong, and frequent rockburst and dynamic roof-fall accidents occur [4, 5], which causes many casualties and serious economic losses. On January 17, 2017, a rockburst accident occurred along the goaf of fully mechanized working face 4203 in Danshuigou Coal Mine of China National Coal Group, Shanxi Province; 9 people were killed and the 115 m long roadway was severely damaged (Figure 1). The average mining depth of working face 4203 was about 400 m, and the inappropriate design of a coal pillar of 20 m wide led to concentration of stress, which was the main cause of the rockburst accident.

If the design of the sectional coal pillar width along goaf working face in the rockburst mine well is inappropriate, rockbursts and large deformations in the surrounding rock may occur at the same time [6–9]. Many scholars have studied the proper width of coal pillars. Liu et al. [10] utilized field monitoring, theoretical calculation, and numerical simulation to investigate the distribution characteristics of lateral bearing pressure of fully mechanized working face in goaf of deep mine thick coal seams and proposed that four factors needed to be taken into account when determining

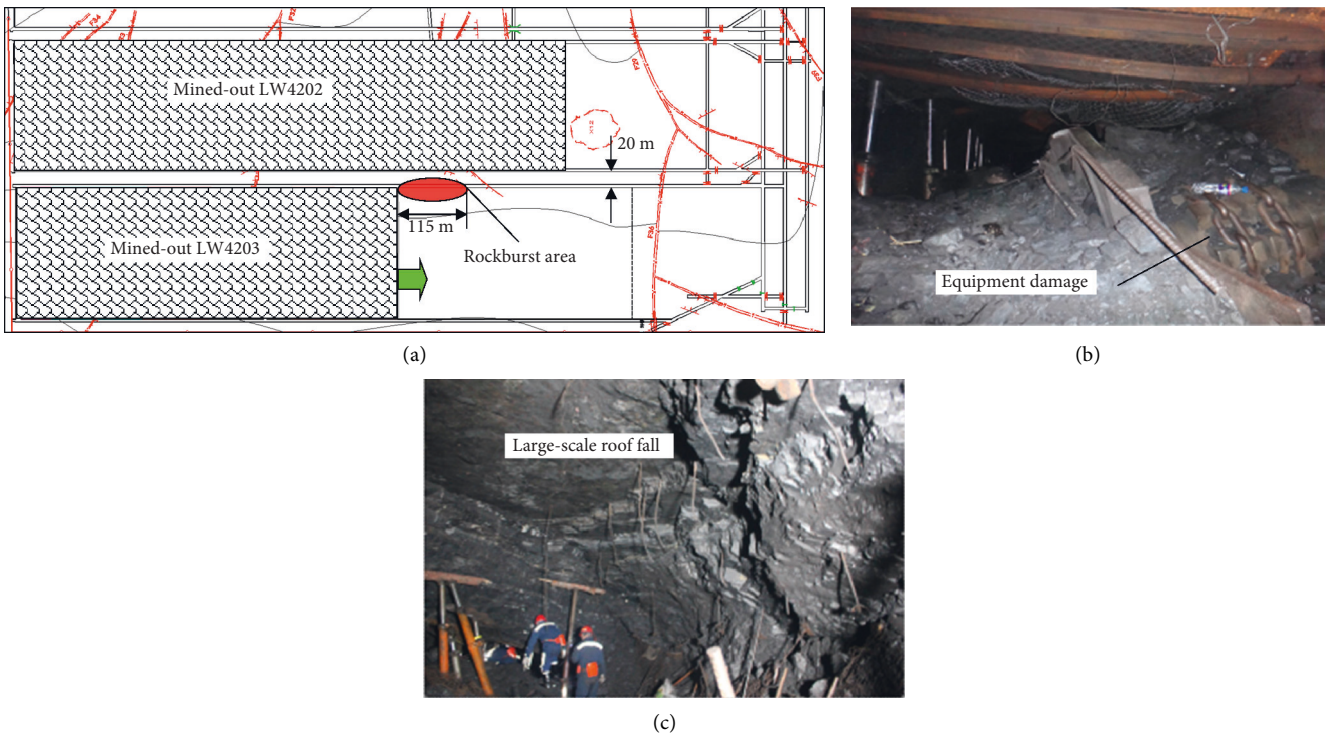

Figure 1: Rockburst photos of gob-side entry in Danshuigou Coal Mine: (a) plane position map of working face; (b) field photo of equipment damage; (c) field photo of roof fall.

sectional coal width. Hauquin T et al. [11] analyzed how an explicit numerical modelling method may be used to calculate and locate the damping of this kinetic energy during pillar failure. Cao et al. [12] studied the microseismic multidimensional information for the identification of rock bursts and spatial–temporal pre-warning in a specific coalface which suffered high rock burst risk in a mining area near a large residual coal pillar. Li et al. [13] studied the characteristic strata movement and mechanism underlying fault–pillar induced rock bursts (FPIRBs) and proposed that the most important factors affecting FPIRB are the static stress in the pillar and the dynamic stress induced by fault slides. Das AJ et al. [14] developed a generalised analytical solutions to estimate the strength of the coal pillars which can be applied for both the inclined and flat coal pillars. Jaiswal A et al. [15] describes an approach to estimation of strain-softening constitutive behaviour of coal-mass through calibration of a numerical model with field cases. Qin et al. [16] analyzed the relationship between the width of coal pillar and its permeability under the premise of stability and proposed an equation for the calculation of proper coal pillar width for preventing spontaneous combustion of coal pillar. Zhao et al. [17] carried out research and showed that the stability of coal pillar was mainly affected by the top main roof and multiple mining activities. With the increase of coal pillar width, the stress concentration zone shifted from the solid coal laterally to the middle of coal pillar. Li et al. [18] studied the stress distribution rules of sectional coal pillars under various buried depth and dip angles. When the dip angle of coal seam increased, the extent of stress concentration was more apparent. These scholars studied the distribution rules of bearing pressure in working face and sectional coal pillar width, but most were based on numerical simulation and field monitoring.

This paper is based on the coal pillar in the sectional fully mechanized working face (4-5)04 in an inclined thick coal seam in Liuhuanggou coal mine of Xinjiang Autonomous Region, China. Based on the rock mass test [19, 20], through theoretical calculation [21–23], field monitoring [24], and numerical simulation [25], we determined the appropriate width of coal pillars, and this work may provide reference information for determining the sectional coal width of mine wells like the engineering conditions in the Xinjiang area.

2. Conditions of setting wide sectional coal pillars in Liuhuanggou coal mine

2.1. General conditions of the working face. Working face (4-5)04 of Liuhuanggou coal mine of Xinjiang is a gob-side working face with an average strike length of 2,636 m and incline width of 180 m. The main mining seam, seam 4-5, has a thickness of 6.06 m to 7.52 m and average thickness of 6.15 m. The dip angle is 21–26° with an average value of 25°. Figure 2(a) shows the plane position map of working face (4-5)04, which sets a 40 m wide sectional coal pillar to isolate goal (4-5)02. Figure 2(b) shows the section plan. The rock structure of the working face is provided in Table 1. As per the appraisal conclusion of rockburst tendency in seam 4-5 of Liuhuanggou coal mine, seam 4-5 was found to have a weak rockburst tendency, as shown in Table 2.

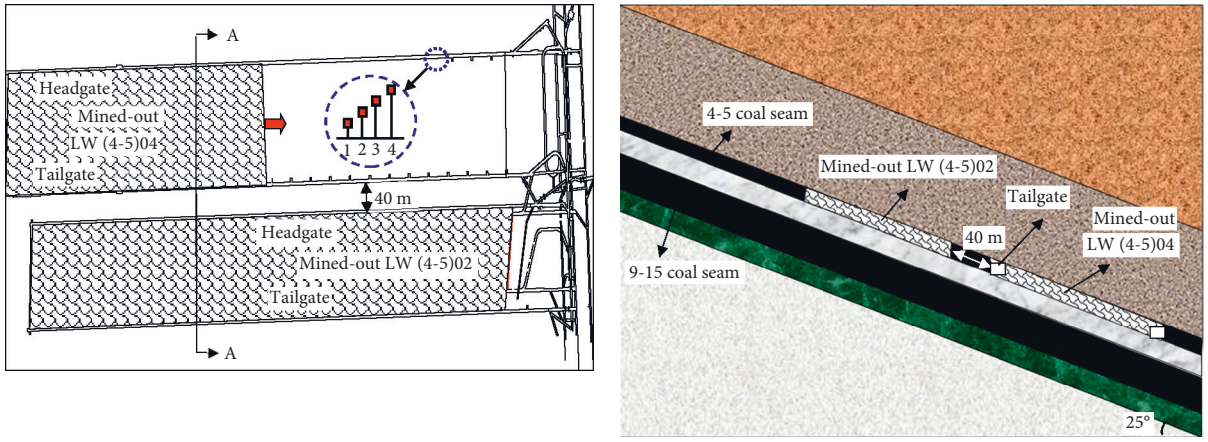

(a) (b)

Figure 2: Cross-section detail of LW (4-5)04: (a) plane position map of working face; (b) A-A Section.

Table 1: Rock structure of borehole in LW (4-5)04.

Rock stratum number (13-2S)	Lithology	Thickness (m)
R_{10}	Medium sandstone	3.7
R_9	Siltstone	5.9
R_8	Mudstone	3.4
R_7	Coal seam 4-5	6.3
R_6	Mudstone	2.9
R_5	Coal seam 7	2.5
R_4	Fine sandstone	2.9
R_3	Siltstone	2.3
R_2	Fine sandstone	2.6
R_1	Siltstone	5.4
Coal	Coal seam 9-15	38
F_1	Mudstone	3.55

Table 2: Appraisal results of coal seam 4-5 rockburst tendency.

Category	Dynamic failure time (ms)	Rockburst energy index	Elastic energy index	Uniaxial compressive strength (MPa)
Average	260	1.10	32.13	13.34
Determination of rockburst tendency	Weak	None	Strong	Weak
Comprehensive determination result			Weak	

2.2. Mining conditions of wide coal pillars in the working face. After the working face (4-5)04 entered the stage of gob-side mining, the mining pressure in the tailgate became very strong due to the high stress concentration of the 40 m wide coal pillar, and frequent coal bursts resulted in a larger mining roof subsidence (Figure 3(a)). The large-diameter boreholes on the side of the coal pillar tended to close (Figure 3(b)). For this reason, establishing a properly sized sectional coal pillar, dispersing the coal pillar stress, and the deformation of surrounding rock in gob-side entry could significantly improve mining safety of the working face in seam 4-5 in Liuhuanggou coal mines.

2.3. Study concept. Our observations of the patterns of pressure in the Liuhuanggou coal mine show that the recovery of coal resources, the stability of roadway surrounding rock, and the prevention of rockburst and secondary disaster (such as flood, fire, and marsh gas) in adjacent goaf should be taken into account when determining the proper sectional coal pillar width. Of these, the stability and rockburst risk of surrounding rock in gob-side entry are related to the stress condition, and the recovery of coal resource and the prevention of secondary disaster in adjacent goaf are related to the width and integrity of coal pillar. This paper first studies the characteristics of lateral bearing pressure distribution in goaf of a fully mechanized working face in inclined thick coal seams, to determine the range of the low stress zone; then, the integrity of coal body in low stress zone is divided to ensure that the gob-side entry is not affected by high lateral stress and a secondary disaster in the goaf.

(a) (b)

Figure 3: Field photos of rail groove in working face (4-5)04: (a) heavy roof subsidence; (b) Borehole Deformation.

3. Theoretical calculation of lateral bearing pressure distribution in goaf of inclined thick coal seam

3.1. Theoretical calculation model. According to the monitoring results from the ground subsidence in Liuhuanggou coal mine, the ground subsidence coefficient after mining of working face (4-5)04 is only 0.1. This meant that it was in the incomplete mining stage, and the overlying rock in goaf is still in an overhanging state. Based on the monitoring results from ground subsidence, this research established a lateral bearing pressure estimation model in goaf of fully mechanized working face in inclined thick coal seam, as shown in Figure 4.

When the rock is in incomplete mining stage after mining of working face, the rock rupture height is approximately half of the width of goaf [26]. Because the overlying strata of both sides of the goaf are in the state of overhanging, half of the weight of the overhanging rock will act as a load on one side of the coal body in the goaf. The angles β and θ between the horizontal direction and the lines that connect the goaf and the stratum end are the rock stratum angular displacements.

The later bearing pressure σ on one side of coal body in goaf consists of self-weight stress σ_q and stress increment $\Delta\sigma$, i.e.,

$$\sigma = \Delta\sigma + \sigma_q, \tag{1}$$

where $\Delta\sigma$ equals to the sum of the pressure transferred to one side of the coal body by the hanging parts of the key layers above the goaf, i.e., $\Delta\sigma = \Sigma\sigma_i$; σ_i is the pressure transferred to one side of coal body from the hanging part of the ith layer; $i = 1{\sim}n$, n is the number of key layers above goaf.

The weight of each key layer of suspended coal transferring to one side of the goaf is half its weight, and the stress increment transferred to one side of the goaf is approximately in isosceles triangle distribution as shown in Figure 4. Therefore, the stress increment transferred to one side of coal body in goaf from the ith key layer is as follows:

$$\Delta\sigma = \begin{cases} 2\sigma_{\max i}\dfrac{x}{S_i}, & \left(0 \le x < \dfrac{S_i}{2}\right), \\ 2\sigma_{\max i}\left(1 - \dfrac{x}{S_i}\right), & \left(\dfrac{S_i}{2} \le x < S_i\right), \\ 0, & x \ge S_i. \end{cases} \tag{2}$$

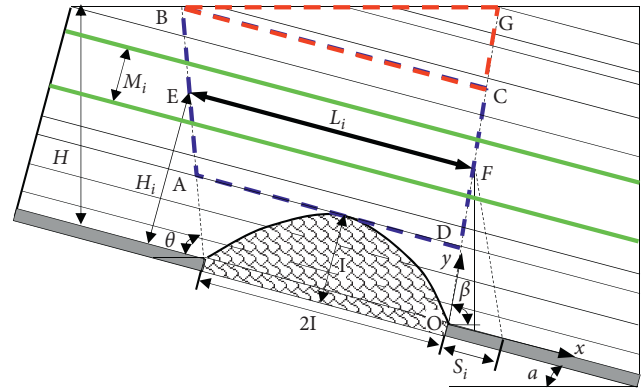

Figure 4: Theoretical calculation model

Here, $\sigma_{\max i}$ is the maximum bearing pressure on one side of coal body in goaf produced by the ith key layer; $\sigma_{\max i} = 2Q_i/S_i$; M_i is the thickness of the ith key layer; and S_i is the influential distance of transferring stress from the ith key layer.

The weight Q_i of each key layer is the sum of its self-weight and the weight of its controlled weak rock layer. The weight transferred from the key layer to one side of coal body is half of its weight, i.e.,

$$Q_i = \frac{q_i}{2} = \frac{\gamma L_i (M_i + m_i)}{2}. \tag{3}$$

Here, Q_i represents the weight transferred from key layer to one side of coal body in goaf; $i = 1 - n$, n is the number of key layers above coal layer; γ represents the bulky density of rock; L_i is the overhang length for the thickness center of the ith key layer locating in goaf, and $L_i = 2I + H_i\cot\theta - H_i\tan(\alpha + \beta - \pi/)2$. H_i is the distance from the thickness center of the ith key layer to the coal floor, and $H_i = I + M_i/2 + \Sigma M_j (j = 1 \ldots i - 1)$; $2I$ is the width of goaf; M_i and m_i are the thickness of the ith key layer and its controlled rock layer, respectively; γ is the bulky density of rock.

Because the $\triangle BCG$ part of the overlying rock in the inclined coal seam cannot form the rock beam structure to transfer the load to the front of the coal wall, the weight of the rock beam structure should be borne by the uppermost key layer of the working face. Then the weight transferred onto the coal body from the nth key layer is as follows:

$$Q_n = \gamma\left(L_n M_n + Q_{\triangle BCG}\right). \tag{4}$$

The area of ΔBCG part from the overly rock layer is as follows:

$$S_{\Delta BCG} = \frac{(BC \times GC \times \sin \angle BCG)}{2}. \tag{5}$$

According to the trigonometric function relation in Figure 4, the range of influence S_i of the key layer from the ith layer on the lateral coal seam in goaf is obtained by the following:

$$S_i = \frac{2H_i \cos \beta}{\cos(\alpha + \beta - (\pi/2))}\left[\cos \alpha + \frac{\sin \alpha}{\tan(\beta - \alpha)}\right]. \tag{6}$$

The stress increment from n critical layers is superposed and the stress increment $\Delta\sigma$ is obtained.

The stress σ_q produced by self-weight is as follows:

$$\sigma_q = \begin{cases} \gamma I, & \left(x = 0 \longrightarrow \dfrac{I \cos \alpha \cos \beta}{\cos(\alpha + \beta - (\pi/2))}\right), \\ \gamma x \dfrac{\cos(\alpha + \beta - (\pi/2))}{\cos \alpha \cos \beta}, & \left(x = \dfrac{I \cos \alpha \cos \beta}{\cos(\alpha + \beta - (\pi/2))} \longrightarrow \dfrac{H \cos \alpha \cos \beta}{\cos(\alpha + \beta - (\pi/2))}\right), \\ \gamma H, & \left(x = \dfrac{H \cos \alpha \cos \beta}{\cos(\alpha + \beta - (\pi/2))} \longrightarrow \infty\right), \end{cases} \tag{7}$$

where H is mining depth.

3.2. Calculation results. Because the overlying rock of seam 4-5 was mostly hard sandstone, according to the statistical results from borehole 27-2 near the working face, from seam 4-5 to the surface of the rock roof, the thickness of sandstone formation accounted for 96% of overall rock thickness. Considering the larger hardness and thickness of the overlying rock, to simplify the calculation process, the rock layer above the fracture range in goaf was calculated as one rock formation, and its thickness M1 was 309 m. According to the practical conditions of working face (4-5)04, the dip angle of coal seam was selected as $\alpha = 25^\circ$, the rock stratum angular displacement under the working face was $\beta = 85^\circ$, the rock stratum angular displacement above the working face was $\theta = 80^\circ$, the mining depth of the tailgate in working face was 440 m, the mining depth of headgate was 500 m, the inclined length of working face was 2I=180 m, and the bulky density of rock γ is 25 kN/m^3. Substitute these parameters into Equation (1) through Equation (7) and calculate the lateral bearing pressure distribution curves for the lower side of goaf in working face (4-5)04 as shown in Figure 5.

The red dotted line in Figure 5 represents strong rockburst risk. The determination basis was that the vertical stress in coal should be 2.0 times greater than the uniaxial compressive strength of coal [27]. As shown, the range of influence of lateral bearing pressure in goaf was approximately 52 m (OD section); the peak value of lateral bearing pressure in goaf was about 26 m (OB section) away from the goaf; the location 12 m to 45 m (AC section) away from the goaf was the high rockburst risk zone, and mining should not be performed in this range; OA section was a low rockburst risk zone (relative low stress zone), and its width is about 12 m (arranging mining roadway within this range needs to consider the dynamic stress issues during mining).

4. Field measurement of lateral bearing pressure distribution in goaf of inclined thick coal seam

To understand the characteristics of lateral bearing pressure of coal body in goaf during mining, the real monitoring alert system of rockburst was adopted to monitor the characteristics of the variations in bearing pressure of the heading side coal body in headgate of working face (4-5)04. One group of stress measurement stations was arranged in the headgate heading side from 46 m of advanced working face (4-5)04. Four stress gauges were installed at 4 m, 7 m, 12 m, and 16 m from the roadway (Figure 1). The boreholes were parallel to dip angle of coal seam.

These stress measurement stations started their monitoring service on April 12, 2017 (from 46 m of advanced working face). The monitoring ended on May 16, 2017 (entering 85 m of goaf) after 35 days of continuous monitoring. Figure 6 shows the relative stress variation curves of coal body. The distance below date showed the distance between working face and stress measurement station. Positive values indicate that the stress measurement station was located ahead of the working face and negative values indicate the stress measurement station was located behind the working face and had entered the goaf.

It was found from Figure 6 that the stress gauge at the 4 m deep measurement point began to continuously drop from 7.3 MPa to the minimum 0.42 MPa after the working face entered 13.5 m in goaf (April 25). The main reason was that the roof rotary compression caused the yield failure of the shallow coal seam, and the slow rise of stress later was due to the recovery of the stress in shallow coal body caused by the continuous rotary compression of the roof in the goaf. After the stress values at the 7 m and 12 m deep measurement points stabilized at the initial installation period,

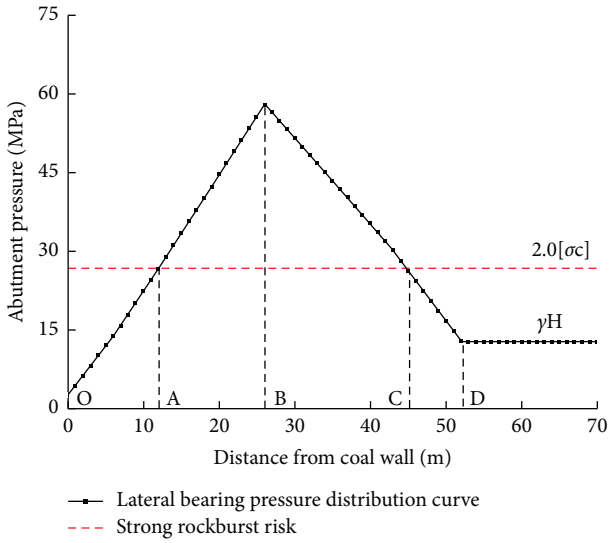

Figure 5: Lateral bearing pressure curve in goaf of working face (4-5)04

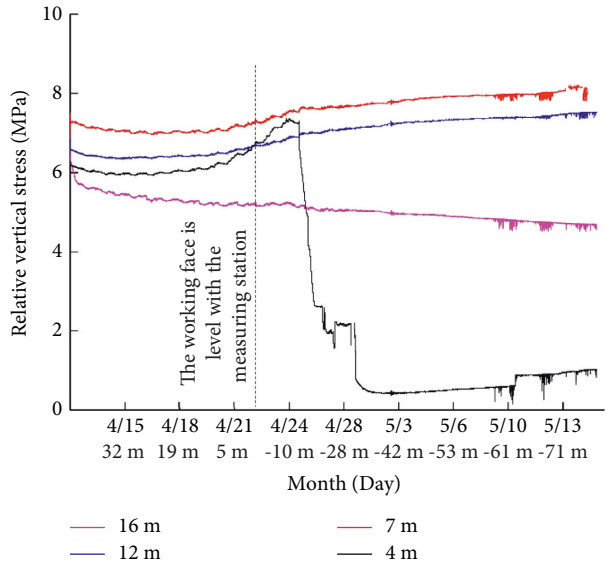

Figure 6: Variation curve of relative vertical stress of coal

both stress curves exhibited a steady increasing tendency. This meant that two measurement points were located within the rotary influential range of lateral rock failure in goaf; the stress curve at the 16 m deep measurement point kept slowly decreasing tendency after installation. This meant that the lateral rock fracture position was in 16 m. Therefore, the lateral fracture position of the main roof of working face (4-5)04 was located between 12 m and 16 m, i.e. average lateral low stress range in goaf was 14 m.

5. Numerical simulation of lateral bearing pressure distribution in goaf of inclined thick coal seam

A numerical calculation model was established based on the geological and mining conditions of the working face (4-5)04 in Liuhuanggou mine, and the model size was length × width × height = 571 × 500 × 415 m with 161,387 nodes and element cells of 152,550 as shown in Figure 7. The four sides and bottom were displacement boundary. The 90 m high rock weight between model top to ground was substituted by applying 2.25 MPa distribution loading. The model calculation utilized Mohr-Coulomb criterion. The physical and mechanical parameters of the rock were obtained from the geological report and borehole data of the mine.

Mining of working faces (4-5)02 and (4-5)04 was simulated to resemble the actual mining situation of Liuhuanggou mine. The vertical stress distribution cloud map and plastic zone after mining completion of two working faces were presented in Figure 8 (partial enlarged detail).

As shown in Figure 8, after mining completion of working faces (4-5)02 and (4-5)04, 40 m wide sectional coal pillar exhibited a higher stress concentration, and there was apparent elastic core, which was the main source of mining pressure in the track grooves in the working face (4-5)04 and the headgates in (4-5)06 and large deformation of surrounding rock. The low stress zone width of the down side in the goaf of working face (4-5)04 was approximately 10 m, and the results of numerical simulation were consistent with those of theoretical calculation.

6. Determination of proper width of coal pillar in fully mechanized working face of inclined thick coal seam

6.1. Determination of lateral low stress zone range. The range of influence and peak position of bearing pressure obtained by theoretical calculation, stress monitoring, and numerical simulation are summarized in Table 3. By summarizing stress monitoring, theoretical calculation, and numerical simulation results, the width of low stress zone of the lateral bearing pressure in the goaf of the upper working face was determined to be 12 m.

6.2. Determination of sectional coal pillar width. The determination of sectional coal pillar width must consider the stability of gob-side entry. For this reason, the gob-side entry should be arranged within 12 m of goaf sides. From the viewpoints of controlling flooding, fire, gas, and other secondary disasters, the width of sectional coal pillar must be greater than 3 m. With consideration of the effectiveness of anchoring bearing (anchoring rod has a length of 2.2 m in field), the width of coal pillar should not be less than 3 m. From the viewpoint of preventing rockbursts during mining of working face, the width of low stress protection zone for gob-side entry solid side should not be less than 4 m, and given a 4 m wide gob-side entry, the width of sectional coal pillar should not be less than 5 m. Through comprehensive analysis, a proper coal pillar width for roadway protection should be between 3 m and 5 m.

6.3. Construction validation. Working face (4-5)06 of Liuhuanggou mine was mined forward along gob-side entry. Considering the fact that there was no experience in

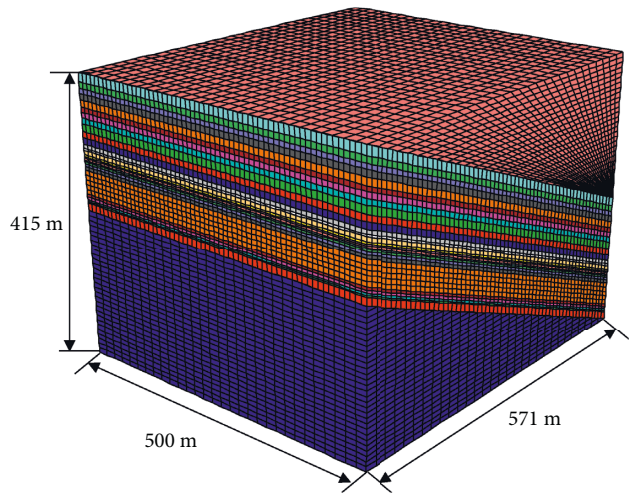

Figure 7: Numerical calculation model

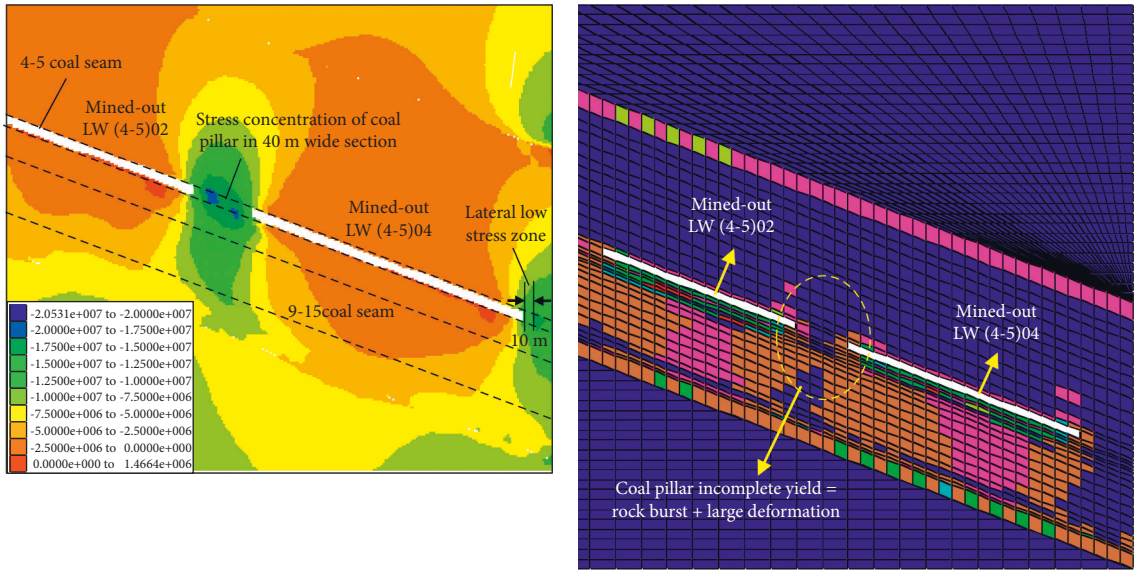

(a) (b)

Figure 8: Numerical simulation results: (a) cloud map of vertical stress (unit: Pa); (b) profile of plastic zone distribution.

Table 3: Comparison between theoretical calculation, stress monitoring and numerical simulation results.

Method	Range of lateral low stress zone (m)	Position of peak lateral bearing pressure (m)
Stress monitoring	12–16 (average 14)	--
Numerical simulation	10	--
Theoretical calculation	12	26
Average value	12	26

forwarding mining along gob-side entry for this mine well and adjacent mine wells, and severe disasters of flooding, fire and gas in goaf of mine wells, the sectional coal pillar width at the initial period of forwarding mining in gob-side entry was enlarged to 7 m. During mining, there was intense mining pressure. There were head-on entry explosions and frequent breakage of the anchor cable. The displacement on the two sides of entry, roof and floor all exceeded 500 mm (Figure 9(a)). The main cause was that a larger sectional coal pillar width resulted in the gob-side entry entering the lateral high stress range of goaf. The mining construction party later accepted the advice to reduce the sectional coal pillar width to 4 m, and both mining pressure and surrounding rock deformation greatly decreased (Figure 9(b)).

Therefore, according to the field pressure behavior of roadway along the gob and the control requirement of surrounding rock deformation, it is appropriated to have the width of coal pillar around 4 m.

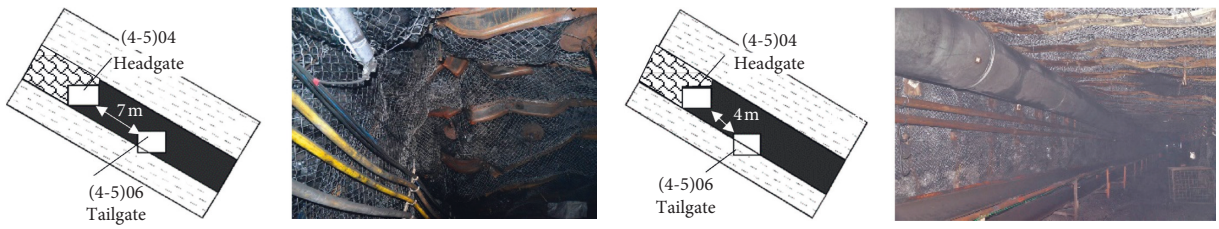

(a) (b)

Figure 9: Field photos of gob-side entry for various sectional coal pillar widths: (a) sectional coal pillar width 7 m; (b) sectional coal pillar width 4 m

7. Conclusion

Based on pre-setting the sectional coal pillar in fully mechanized working face of an inclined coal seam of Liuhuanggou coal mine, this research studied the proper sectional coal pillar width in fully mechanized working face in inclined thick coal seam by means of theoretical analysis, stress monitoring, and numerical simulation and reached the following main conclusions:

(1) Through establishing the theoretical calculation model of lateral bearing pressure in goaf of inclined thick coal seam, this research concluded that the influence range of lateral bearing pressure in the goaf of working face (4-5)04 was about 52 m; the peak value position of lateral bearing pressure in goaf was about 26 m away from the goaf; the location 12 m to 45 m away from the goaf was high rockburst risk zone, and mining construction cannot be arranged within this range.

(2) By summarizing the stress monitoring, theoretical calculation, and numerical simulation results, we here concluded that the width of low stress zone for the lateral bearing pressure in upper working face was 12 m. With consideration of prevention of secondary disasters in goaf, roadway bearing, and rockburst prevention, the proper width of sectional coal pillar for working face (4-5)06 was finally found to be between 3 m to 5 m.

(3) Field practice showed that the determined sectional coal pillar was appropriate. When the sectional coal pillar was too large, rockburst and large deformation of surrounding rock could occur simultaneously; so field construction should strictly control the sectional coal pillar width.

Data Availability

The data used to support the findings of this study are available from the corresponding author upon request.

Conflicts of Interest

The authors declare that there are no conflicts of interest regarding the publication of this paper.

Acknowledgments

The authors gratefully acknowledge financial support from the National Natural Science Foundation of China (Grant No. 51874133, 51674014, 51904017, 51634001) and Engineering Research Center of Geothermal Resources Development Technology and Equipment, Ministry of Education, Jilin University (No. 21013). The authors also thank Liuhuanggou Coal Mine for support and assistance during field verification and application.

References

[1] Z. Yang, C. Liu, S. Tang, L. Dou, and J. Cao, "Rock burst mechanism analysis in an advanced segment of gob-side entry under different dip angles of the seam and prevention technology," *International Journal of Mining Science and Technology*, vol. 28, no. 6, pp. 55–63, 2018.

[2] Z. L. Li, X. Q. He, L. M. Dou, and Dz Song, "Comparison of rockburst occurrence during extraction of thick coal seams using top-coal caving versus slicing mining methods," *Canadian Geotechnical Journal*, vol. 55, no. 10, pp. 1433–1450, 2018.

[3] P. Konicek and J. Schreiber, "Heavy rockbursts due to longwall mining near protective pillars: a case study," *International Journal of Mining Science and Technology*, vol. 28, pp. 799–805, 2018.

[4] B. María, "Aguado. Díaz, C. González, "Influence of the stress state in a coal bump-prone deep coalbed: a case study," *International Journal of Rock Mechanics and Mining Sciences*, vol. 46, no. 2, pp. 333–345, 2009.

[5] G. Bräuner, *Rockbursts in Coal Mines and Their Prevention*, Routledge, England, UK, 2017.

[6] S. T. Zhu, F. X. Jiang, and J. H. Liu, "Research on mechanism of rock burst and large deformation coordination controlling in thick coal seam of deep shaft," *Chinese Journal of Rock Mechanics and Engineering*, vol. 34, no. S2, pp. 4262–4268, 2015.

[7] S. T. Zhu, Y. Feng, F. X. Jiang, and J. Liu, "Mechanism and risk assessment of overall-instability-induced rockbursts in deep island longwall panels," *International Journal of Rock Mechanics and Mining Sciences*, vol. 106, pp. 342–349, 2018.

[8] Q. Wang, S. Xu, Z. Xin, M. He, H. Wei, and B. Jiang, "Mechanical properties and field application of constant resistance energy-absorbing anchor cable," *Tunnelling and Underground Space Technology*, vol. 125, Article ID 104526, 2022.

[9] Q. Wang, S. Xu, M. C. He, B. Jiang, H. Wei, and Y. Wang, "Dynamic mechanical characteristics and application of

constant resistance energy-absorbing supporting material," *International Journal of Mining Science and Technology*, vol. 32, no. 3, pp. 447–458, 2022.

[10] J. H. Liu, F. X. Jiang, and N. G. Wang, "Survey on abutment pressure distribution of fully mechanized cavingface in extra-thick coal seam of deep shaft," *Journal of China Coal Society*, vol. 36, no. S1, pp. 18–22, 2011.

[11] T. Hauquin, Y. Gunzburger, and O. Deck, "Predicting pillar burst by an explicit modelling of kinetic energy," *International Journal of Rock Mechanics and Mining Sciences*, vol. 107, pp. 159–171, 2018.

[12] A. Y. Cao, L. M. Dou, C. B. Wang, Xx Yao, Jy Dong, and Y. Gu, "Microseismic precursory characteristics of rock burst hazard in mining areas near a large residual coal pillar: a case study from xuzhuang coal mine, xuzhou, China," *Rock Mechanics and Rock Engineering*, vol. 49, pp. 4407–4422, 2016.

[13] Z. L. Li, L. M. Dou, W. Cai et al., "Investigation and analysis of the rock burst mechanism induced within fault–pillars," *International Journal of Rock Mechanics and Mining Sciences*, vol. 70, pp. 192–200, 2014.

[14] A. J. Das, P. K. Mandal, P. S. Paul, and R. K. Sinha, "Generalised analytical models for the strength of the inclined as well as the flat coal pillars using rock mass failure criterion," *Rock Mechanics and Rock Engineering*, vol. 52, pp. 3921–3946, 2019.

[15] A. Jaiswal and B. K. Shrivastva, "Numerical simulation of coal pillar strength," *International Journal of Rock Mechanics and Mining Sciences*, vol. 46, pp. 779–788, 2009.

[16] R. X. Qin, K. Yang, and S. Liu, "Study on permeability and fire proof effectiveness of sectional coal pillar," *Journal of Mining and Safety Engineering*, vol. 35, no. 3, pp. 629–634, 2018.

[17] B. Zhao, F. T. Wang, and N. N. Liang, "Reasonable segment pillar width and its control technology for fully mechanized top-coal caving face with high stress," *Journal of Mining & Safety Engineering*, vol. 35, no. 1, pp. 19–26, 2018.

[18] X. J. Li, H. Z. Li, and R. F. Yuan, "Stress distribution influence on segment coal pillar at different dip angles of working face," *Journal of China Coal Society*, vol. 37, no. 8, pp. 1270–1274, 2012.

[19] Y. Q. Su, F. Q. Gong, S. Luo, and Zx Liu, "Experimental study on energy storage and dissipation characteristics of granite under two-dimensional compression with constant confining pressure," *Journal of Central South University*, vol. 28, no. 3, pp. 848–865, 2021.

[20] Z. J. Wu, Z. Y. Wang, L. F. Fan, L. Weng, and Qs Liu, "Micro-failure process and failure mechanism of brittle rock under uniaxial compression using continuous real-time wave velocity measurement," *Journal of Central South University*, vol. 28, pp. 556–571, 2021.

[21] D. H. Chen, H. E. Chen, W. Zhang, J. Lou, and B. Shan, "An analytical solution of equivalent elastic modulus considering confining stress and its variables sensitivity analysis for fractured rock masses," *Journal of Rock Mechanics and Geotechnical Engineering*, vol. 14, no. 3, pp. 825–836, 2022.

[22] M. Z. Gao, J. Xie, J. Guo, Y. Lu, Z. He, and C. Li, "Fractal evolution and connectivity characteristics of mining-induced crack networks in coal masses at different depths," *Geomechanics and Geophysics for Geo-Energy and Geo-Resources*, vol. 7, no. 1, Article ID 9, 2021.

[23] M. M. He, Z. Q. Zhang, J. W. Zhu, and N. Li, "Correlation between the constant m(i) of hoek-Brown criterion and porosity of intact rock," *Rock Mechanics and Rock Engineering*, vol. 55, pp. 923–936, 2022.

[24] W. Xiao, J. C. Li, X. B. Zhao, and Y. Liang, "Propagation characteristics and prediction of blast-induced vibration on closely spaced rock tunnels," *Tunnelling and Underground Space Technology*, vol. 123, Article ID 104416, 2022.

[25] P. Zhang, D. F. Zhang, and Y. Yang, "A case study on intergrated modeling of spatial information of a complex geological body," *Lithosphere*, vol. 2022, Article ID 2918401, 10 pages, 2022.

[26] F. X. Jiang, S. H. Yang, and L. Xun, "Spatial fracturing progresses of surrounding rock masses in longwall face monitored by microseismic monitoring techniques," *Journal of China Coal Society*, vol. 2003, no. 04, pp. 357–360, 2003.

[27] G. Y. Yang, *Partition Prevention and Control of Rock Burst at the Headgate of Ultra-thick Coal Seam*, University of Science and Technology Beijing, Beijing, China, 2019.